URaG: Unified Retrieval and Generation in Multimodal LLMs for Efficient Long Document Understanding

Yongxin Shi[1*]**, Jiapeng Wang**[1*]**, Zeyu Shan**[1]**, Dezhi Peng**[2†]**, Zening Lin**[1]**, Lianwen Jin**[1 †]**,**

[1]South China University of Technology
[2]Huawei Technologies Co., Ltd.
yongxin_shi@foxmail.com, eelwjin@scut.edu.cn

Abstract

Recent multimodal large language models (MLLMs) still struggle with long document understanding due to two fundamental challenges: information interference from abundant irrelevant content, and the quadratic computational cost of Transformer-based architectures. Existing approaches primarily fall into two categories: token compression, which sacrifices fine-grained details; and introducing external retrievers, which increase system complexity and prevent end-to-end optimization. To address these issues, we conduct an in-depth analysis and observe that MLLMs exhibit a human-like coarse-to-fine reasoning pattern: early Transformer layers attend broadly across the document, while deeper layers focus on relevant evidence pages. Motivated by this insight, we posit that the inherent evidence localization capabilities of MLLMs can be explicitly leveraged to perform retrieval during the reasoning process, facilitating efficient long document understanding. To this end, we propose **URaG**, a simple-yet-effective framework that Unifies Retrieval and Generation within a single MLLM. URaG introduces a lightweight cross-modal retrieval module that converts the early Transformer layers into an efficient evidence selector, identifying and preserving the most relevant pages while discarding irrelevant content. This design enables the deeper layers to concentrate computational resources on pertinent information, improving both accuracy and efficiency. Extensive experiments demonstrate that URaG achieves state-of-the-art performance while reducing computational overhead by 44-56%. The code is available at https://github.com/shi-yx/URaG.

Introduction

Document understanding plays a pivotal role in a wide range of real-world applications, such as information extraction, contract analysis, and report processing. While recent multimodal large language models (MLLMs) have shown impressive performance in processing single-page documents (Zhu et al. 2025; Bai et al. 2025), the transition from single-page to multi-page document understanding introduces fundamental scalability and efficiency challenges that remain largely unresolved. The main challenges are twofold. First,
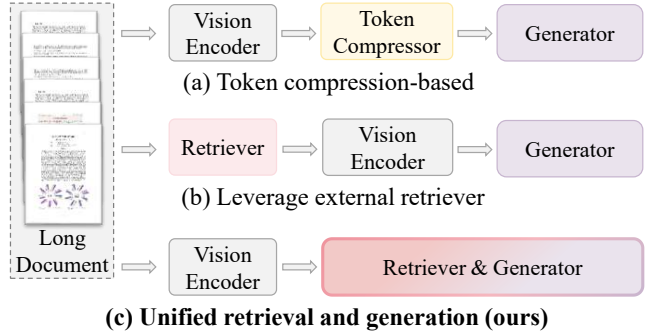

Figure 1: Comparison of different methods for long document understanding. Our method unifies retrieval and generation within a single MLLM, leveraging early-layer features for evidence retrieval during reasoning, which achieves efficient and accurate long document understanding.

the presence of a large volume of irrelevant content often leads to information interference. Second, due to the quadratic computational complexity of Transformer-based architectures with respect to sequence length, processing excessively long sequences results in prohibitively high computational costs, significantly limiting the scalability of existing approaches.

To address these challenges, existing MLLM-based approaches primarily follow two technical routes: (1) The first route involves compressing the input tokens fed into the LLM. These methods (Hu et al. 2024b; Jia et al. 2024) typically apply uniform compression to visual tokens across all pages of the document, thus reducing the token count and alleviating the computational burden. However, this strategy inevitably sacrifices certain visual details during the compression process, potentially impairing the model's capacity for fine-grained visual understanding. (2) The second technical approach involves the introduction of an external retriever. These methods (Zhang, Yu, and Zhang 2024; Chen et al. 2025) employ text-based or vision-based retrievers to extract the most relevant content from long documents, feeding only the retrieved subset into the MLLM. While effective in reducing computational overhead, it introduces high system complexity in real-world deployment, due to the reliance on a separate retrieval module. More importantly, it

lacks end-to-end optimization: Since the retriever is typically trained independently from the MLLM, such systems are prone to suboptimal coordination and error propagation.

When processing long documents, humans rarely read every word carefully and sequentially. Instead, they adopt a coarse-to-fine comprehension strategy (León et al. 2019; Zou et al. 2023). (1) Coarse-grained retrieval: Based on an initial understanding of the question (e.g., keywords, intent, and contextual cues), humans first leverage structural features of the document (e.g., layout, titles, and figures) to rapidly identify pages or regions that are likely to contain relevant information. (2) Fine-grained reading: After locating candidate regions, humans engage in detailed reading to extract precise answers. Motivated by this human reading behavior, we hypothesize that MLLMs exhibit a similar coarse-to-fine reasoning pattern when processing long documents. To verify this hypothesis, we conduct a systematic empirical study. Our analysis reveals that attention distribution evolves progressively across the Transformer layers of the LLM component: early layers tend to distribute attention uniformly across pages, whereas deeper layers increasingly concentrate attention on pages containing answer evidence. This shift in attention patterns provides compelling empirical support that MLLMs inherently perform human-like hierarchical reasoning for long document understanding.

Building on this insight, we posit that the inherent evidence localization capabilities of MLLMs can be explicitly leveraged to perform retrieval during the reasoning process, facilitating efficient long document understanding. To this end, we propose a simple-yet-effective framework, **URaG**, which Unifies Retrieval and Generation within a single MLLM. The key innovation of our framework lies in transforming the early layers (e.g., the first 6 layers) of the MLLM into an efficient retrieval system through a lightweight cross-modal retrieval module. This module consists of two linear layers with minimal additional parameters, processes the hidden states of the early layer to extract visual features and textual features from each page and the question, respectively. Using a contextualized late interaction mechanism (Khattab and Zaharia 2020), it computes relevance scores between text and vision to identify the top-k most relevant pages. These selected pages are preserved in the hidden states and propagated to the deeper layers for answer generation, while irrelevant content is discarded. By unifying retrieval and generation within a single model, our framework enables precise evidence localization, which effectively mitigates information interference and substantially reduces computational overhead.

The effectiveness of URaG is extensively verified on several commonly used benchmarks. Without bells and whistles, experimental results show that URaG achieves state-of-the-art performance. In addition, its computational efficiency is also empirically validated, further underscoring its practical advantages in real-world deployment.

In summary, our main contributions are as follows.

- We present a systematic empirical study revealing that MLLMs inherently exhibit a human-like coarse-to-fine reasoning pattern when processing long documents.

- We propose URaG, an elegant framework that seamlessly integrates evidence retrieval and answer generation within a single MLLM, eliminating the need for external retrieval systems. Equipped with a lightweight cross-modal retrieval module, URaG explicitly leverages the inherent evidence localization capabilities of MLLMs to perform efficient and integrated retrieval.

- Extensive experiments demonstrate the effectiveness of our method, which enhances MLLMs' long document comprehension capability while reducing computational overhead by 44-56%.

Related Work

Long Document Understanding

Existing methods for long document understanding can be primarily categorized into encoder-decoder-based and MLLM-based approaches. **Encoder-decoder-based** methods are built upon encoder-decoder Transformer architectures, such as T5 (Raffel et al. 2020). Representative methods include: Hi-VT5 (Tito, Karatzas, and Valveny 2023) summarizes key information from each page into special [PAGE] tokens for hierarchical decoding. GRAM (Blau et al. 2024) integrates local single-page encoding with global document-level layers, using learnable tokens and bias adaptation to enhance cross-page reasoning. RM-T5 (Dong, Kang, and Karatzas 2024) employs recurrent memory to propagate information across pages sequentially. **MLLM-based** methods primarily focus on optimizing the performance of multimodal large language models in long-sequence reasoning, with two main strategies: (1) Compressing input tokens. To alleviate computational costs, these methods focus on compressing the visual inputs before feeding them into the language model. For instance, mPLUG-DocOwl2 (Hu et al. 2024b) introduces a high-resolution DocCompressor module that reduces each document image to 324 tokens. Similarly, Leopard (Jia et al. 2024) proposes an adaptive high-resolution multi-image encoder, which dynamically allocates visual token sequences based on the resolution and aspect ratios of the input images. (2) Incorporating external retrievers. These approaches employ retrieval mechanisms to pre-select relevant content prior to MLLM inference. For example, CREAM (Zhang, Yu, and Zhang 2024) adopts a coarse-to-fine retrieval pipeline that combines embedding-based similarity search, multi-round grouping, and LLM-based re-ranking to extract the most relevant text segments. SV-RAG (Chen et al. 2025) leverages the final hidden states of MLLMs for question-guided evidence retrieval, feeding only the selected content into the model for answer generation. M3DocRAG (Cho et al. 2024) employs a multimodal retriever to identify relevant content prior to the MLLM.

Document Retrieval

Document retrieval approaches can be broadly categorized into text-based and vision-based methods. **Text-Based retrieval** methods typically rely on Optical Character Recognition (OCR) to extract textual content from documents, followed by similarity computation between the extracted text
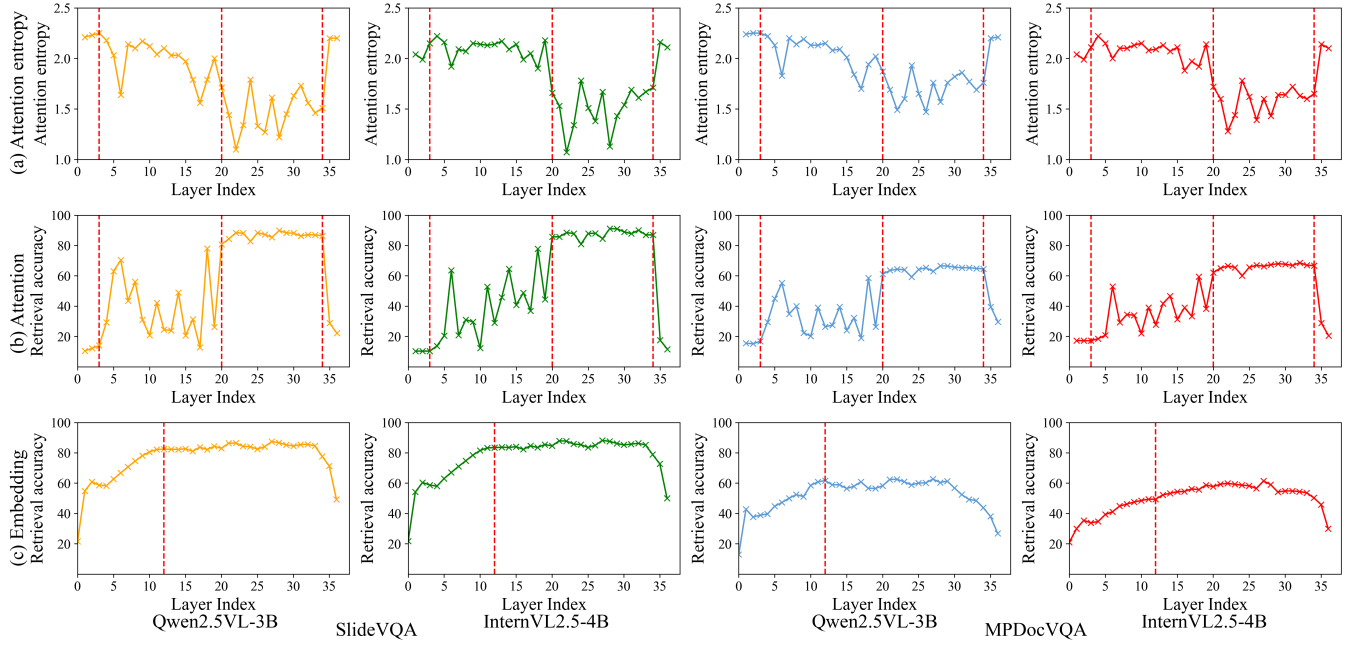
Figure 2: Analysis of MLLMs on long document understanding. (a) Attention entropy. (b) Attention-based retrieval accuracy. (c) Embedding-based retrieval accuracy.

and the query. These methods can be further categorized into sparse and dense retrieval techniques. Widely used sparse retrievers include: TF-IDF (Salton, Fox, and Wu 1983) calculates term relevance using word frequency and inverse document frequency; BM25 (Robertson et al. 1995) improves upon TF-IDF by introducing non-linear term frequency saturation and document length normalization, enhancing ranking robustness. Dense retrieval methods encode text into continuous vector spaces, enabling semantic similarity matching. DPR (Karpukhin et al. 2020) uses a dual-encoder architecture to independently encode questions and passages. SBERT (Reimers and Gurevych 2019) produces sentence-level embeddings via a siamese BERT (Devlin et al. 2019). BGE (Xiao et al. 2024) improves dense retrieval quality through self-knowledge distillation and careful curation of training data. NV-Embed-v2 (Lee et al. 2024) introduces a latent attention-based pooling mechanism for aggregating token representations. **Vision-based retrieval** methods directly encode document images, preserving both textual and layout information. CLIP (Radford et al. 2021) and SigLIP (Zhai et al. 2023) are commonly used to extract retrieval embeddings. Some approaches further leverage MLLMs to jointly encode document images and textual queries for multimodal retrieval. For instance, Col-Pali (Faysse et al. 2025) utilizes PaliGemma (Beyer et al. 2024) to obtain token-level embeddings for each document page. DSE (Ma et al. 2024a) employs Phi-3-V (Abdin et al. 2024) to encode each page into a single dense embedding, facilitating compact yet effective document representation. MM-Embed (Lin et al. 2025) fine-tunes MLLM-based universal multimodal retrievers and prompts pre-trained MLLMs for zero-shot reranking over retrieved candidates.

Analysis

To investigate whether MLLMs exhibit a human-like coarse-to-fine reading behavior, we conduct a systematic empirical study on two representative MLLMs across the subsets of two long document understanding benchmarks. Specifically, we visualize the attention entropy across LLM layers, measuring how the generated tokens attend over input pages, as shown in Figure 2 (a). We further evaluate the retrieval accuracy using attention weights as retrieval scores to identify evidence pages, as shown in Figure 2 (b). In addition, we compute query-to-visual similarity using hidden states from each layer as embeddings, enabling embedding-based retrieval, as shown in Figure 2 (c). From the visualizations and metrics, we observe the following trends: (1) In the early layers (e.g., the first 3 layers), the attention entropy is high and attention-based retrieval accuracy is correspondingly low. This indicates that the model distributes attention relatively uniformly across all pages, reflecting a global and coarse-level reading stage. (2) In the early-middle layers (e.g., layers 3–20), attention entropy exhibits a declining trend with fluctuations, while attention-based retrieval accuracy shows a corresponding upward trend. This suggests the model is progressively attempting to identify and focus on relevant evidence pages. (3) In deeper layers (e.g., layers 20-34), the attention entropy remains low and attention-based retrieval accuracy stays consistently high, indicating a fine-grained reading stage where attention becomes highly concentrated on evidence pages. (4) In the final two layers, attention entropy increases again while attention-based retrieval accuracy slightly drops. This indicates the model revisits all input pages before the final answer, which is similar to how humans recheck the full document to ensure cor-
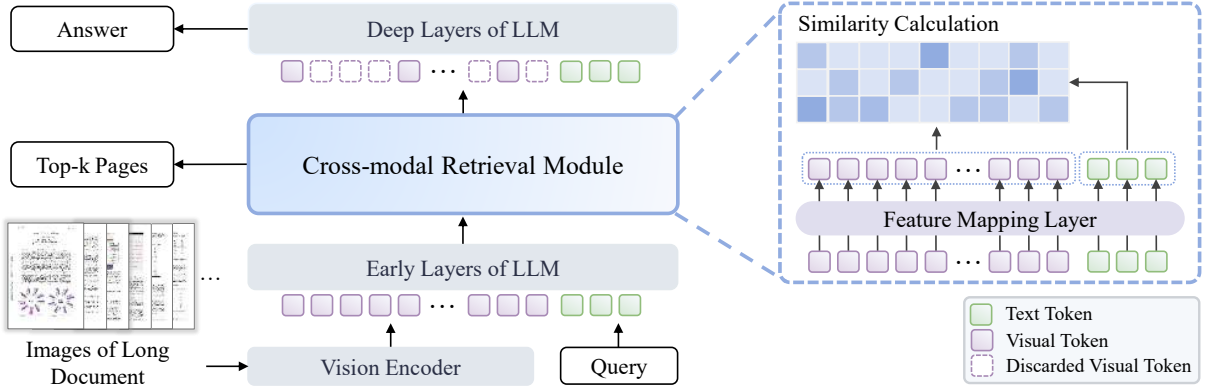
Figure 3: Overview of our URaG framework.

rectness. In summary, these findings provide strong empirical evidence that MLLMs inherently follow a human-like coarse-to-fine reasoning pattern when processing long documents. This insight motivates us to explicitly harness their intrinsic evidence localization ability for unified retrieval-generation approaches.

Moreover, we find that embedding-based retrieval reaches consistently high accuracy (e.g., around layer 12) earlier than attention-based. This implies that semantic representations formed at mid-level layers are already sufficiently discriminative for evidence selection. In addition, embedding-based retrieval shows more stable performance across layers. These two observations motivate us to adopt embedding-based retrieval to develop our method.

Methodology

Framework

The proposed URaG is a unified method that integrates both retrieval and generation within a single model. As illustrated in Figure 3, the framework consists of a multimodal large language model (MLLM) and a lightweight cross-modal retrieval module. Specifically, given a long document composed of pages $\{p_1, p_2, \ldots, p_n\}$, where n denotes the number of pages, and a user query Q, each page image is processed by the vision encoder and the projector to obtain a sequence of visual tokens. The query Q is tokenized by a text tokenizer and then input into the LLM along with the visual tokens. The retrieval module operates on the hidden states from an early layer (the sixth layer in our implementation) of the LLM to retrieve the top-k (k is set to 5 by default) pages most relevant to the query. The visual tokens corresponding to non-retrieved pages are directly discarded from the hidden states. Subsequently, the deeper LLM layers attend only to the retained pages for answer generation.

Cross-modal Retrieval Module

The retrieval module is designed to identify the most relevant pages from multi-page inputs with respect to the query. It is implemented with a lightweight structure consisting of two linear projections with GELU activation. Formally,

given the early-layer hidden states $H \in \mathbb{R}^{L \times D}$, the feature mapping layer is applied to reduce the dimensionality, yielding $H' \in \mathbb{R}^{L \times D'}$, followed by L2 normalization to enhance feature consistency. From H', the visual feature sequences for each document pages $\{E_v^{(1)}, E_v^{(2)}, \ldots, E_v^{(n)}\}$ and the textual feature sequence of the query E_q, are extracted based on positional indices. The similarity between the query text and each document page is computed using the widely adopted contextualized late interaction (Khattab and Zaharia 2020):

$$s_{q,v^{(p)}} = \sum_{i \in [|E_q|]} \max_{j \in [|E_v^{(p)}|]} E_{q_i} \cdot E_{v_j}^{(p)T}. \tag{1}$$

Based on the similarity scores, the top-k pages are retained while others are discarded directly from hidden states, enabling subsequent layers to focus on relevant content, significantly reducing computational overhead.

Training strategy

We adopt a two-stage training strategy to optimize our framework. In the first stage, we pretrain the retrieval module to adapt it for the retrieval task. All model parameters are frozen except for those in the retrieval module, which is optimized using the retrieval loss (Khattab and Zaharia 2020):

$$\mathcal{L}_{\text{retrieval}} = \log\left(1 + \exp(S_{\text{neg}} - S_{\text{pos}})\right), \tag{2}$$

where S_{pos} and S_{neg} represent the scores of positive and negative samples, respectively. They are calculated as follows.

$$S_{\text{pos}} = \sum_{i \in P} s_i \tag{3}$$

$$S_{\text{neg}} = \begin{cases} \sum_{j \in N} s_j & \text{if } N < P \\ \sum_{j \in \text{TopK}(\{s_k | k \in N\}, P)} s_j & \text{if } N \geq P \end{cases} \tag{4}$$

Here, P and N indicate the number of positive and negative samples, respectively, and s denotes the similarity score between the query and a document page.

Method	#Param	SlideVQA		MMLong		DUDE		MPDocVQA	
		Top1	Top5	Top1	Top5	Top1	Top5	Top1	Top5
Text-based									
BM25 (Robertson et al. 1995)	-	69.3	91.1	25.3	47.6	58.4	89.8	59.7	87.8
SBERT (Reimers and Gurevych 2019)	-	73.0	91.0	44.7	70.2	61.7	90.2	67.8	93.3
BGE-M3 (Chen et al. 2024a)	568M	74.3	92.0	42.7	66.6	60.1	90.1	66.8	92.7
BGE-large (Xiao et al. 2024)	326M	81.3	93.3	47.4	71.5	60.1	90.1	66.8	92.7
NV-Embed-v2 (Lee et al. 2024)	7B	82.2	94.3	47.4	69.0	68.8	93.9	74.3	95.2
Vision-based									
CLIP (Radford et al. 2021)	428M	58.4	86.9	32.4	63.4	61.0	89.5	67.8	93.7
SigLIP (Zhai et al. 2023)	878M	66.2	90.1	44.9	69.4	59.4	89.7	64.9	91.9
ColPali (Faysse et al. 2025)	3B	90.2	98.2	60.3	80.2	68.5	93.3	73.6	95.6
MM-Embed (Lin et al. 2025)	7B	70.9	91.8	42.9	74.7	65.6	91.9	69.5	94.0
SV-RAG (Chen et al. 2025)	4B	90.6	98.8	_64.8_	84.8	-	-	-	-
URaG-3B (ours)	3B	_92.1_	_98.9_	63.0	_85.4_	_83.0_	**97.0**	_84.4_	**98.0**
URaG-7B (ours)	7B	**92.9**	**99.0**	**68.3**	**86.0**	**83.9**	_96.9_	**84.5**	**98.0**

Table 1: Retrieval performance comparison with different methods. MMLong refers to MMLongBench-Doc.

In the second stage, the LoRA (Hu et al. 2022) adapter is added to both the LLM and retrieval module, with other parameters kept frozen. The model is jointly optimized through the retrieval loss and generation loss.

$$\mathcal{L}_{\text{total}} = \mathcal{L}_{\text{retrieval}} + \mathcal{L}_{\text{generation}}, \quad (5)$$

where $\mathcal{L}_{\text{generation}}$ is the cross-entropy loss for answer generation. To facilitate adaptation to fine-grained visual features, we retain at most five pages after retrieval. Ground-truth evidence pages are always kept to ensure information completeness, while remaining pages are selected by the highest retrieval scores.

Experiments

Implementation Details

Our model is available in two sizes: URaG-3B and URaG-7B, both built upon Qwen2.5-VL (Bai et al. 2025). The retrieval module consists of two linear projection layers with GELU activation, which sequentially reduce the dimension of hidden states to 1024 and then to 512. The model is trained with a batch size of 4 and 8 gradient accumulation steps with AdamW optimizer. During pretraining, the initial learning rate is set to 1×10^{-4} with a warm-up ratio of 0.03, followed by a cosine decay schedule. For fine-tuning, we adopt LoRA (Hu et al. 2022) with a rank of 32, alpha of 64, and a dropout rate of 0.1. The loss weights of retrieval and generation are set to 1:1. The warm-up and learning rate settings are the same as in pretraining. The datasets for training including MPDocVQA (Tito, Karatzas, and Valveny 2023), DUDE (Van Landeghem et al. 2023), and SlideVQA (Tanaka et al. 2023). Both retrieval pretraining and joint fine-tuning are conducted for 1 epoch, respectively. Following prior work (Xie et al. 2024; Chen et al. 2025), we retain the top-5 pages in the retrieval module by default. All experiments are conducted on 4 NVIDIA A6000 GPUs.

Evaluation Metrics

Following previous work (Chen et al. 2025), the evaluation involves retrieval and generation metrics. The retrieval metrics include Top1 and Top5 accuracy. The generation metrics include *Average Normalized Levenshtein Similarity (ANLS)* (Tito, Karatzas, and Valveny 2023) for MPDocVQA and DUDE, *Exact Match (EM)* (Tanaka et al. 2023) for SlideVQA, *Generalized Accuracy* and *F1-score* (Ma et al. 2024b) for MMLongBench-Doc, and *Generalized Accuracy score* (Deng et al. 2024) for LongDocURL.

Evidence Page Retrieval

We evaluate the evidence retrieval performance of URaG on MPDocVQA (Tito, Karatzas, and Valveny 2023), DUDE (Van Landeghem et al. 2023), SlideVQA (Tanaka et al. 2023), and MMLongBench-Doc (Ma et al. 2024b), and compare it with both the text-based and vision-based retrievers. For text-based methods, we employ Paddle-OCR (Cui et al. 2025) to extract textual content from document images for retrieval, except on MMLongBench-Doc, where the PDF parser is used. As shown in Table 1, our URaG consistently outperforms all compared methods across datasets. This highlights the effectiveness of our integrated retrieval mechanism, which explicitly leverages the inherent capabilities of MLLMs via a lightweight retrieval module, without requiring complex designs or extensive training.

Main Results

We evaluate the performance of URaG on various long document understanding benchmarks, including MPDocVQA, DUDE, SlideVQA, LongDocURL, and MMLongBench-Doc. The results are demonstrated in Table 2 and 3, respectively. Based on the results, we draw the following key conclusions. Firstly, our method demonstrates strong effectiveness in long document understanding, achieving state-of-the-art performance across multiple benchmarks. Notably, our method significantly outperforms previous methods on

Method	#Param	MPDocVQA	DUDE	SlideVQA	LongDocURL
LayoutLMv3 (Huang et al. 2022)	125M	55.1	20.3	-	-
Hi-VT5 (Tito, Karatzas, and Valveny 2023)	316M	61.8	35.7	-	-
DocFormerv2 (Appalaraju et al. 2024)	784M	76.4	48.4	-	-
GRAM (Blau et al. 2024)	859M	83.0	53.4	-	-
Llama-3.2 (Meta AI 2024)	11B	57.6	20.8	-	9.2
LLaVA-Next-Interleave (Li et al. 2024a)	7B	39.9	24.0	-	14.1
Idefics3 (Laurençon et al. 2023)	8B	67.2	38.7	39.9	-
mPLUG-DocOwl2 (Hu et al. 2024b)	8B	69.4	46.7	24.6	5.3
CREAM (Zhang, Yu, and Zhang 2024)	14B	65.3	52.5	-	-
Qwen2-VL (Wang et al. 2024)	7B	82.1	45.9	59.9	30.6
InternVL2.5 (Chen et al. 2024b)	4B	74.9	40.7	45.2	24.1
InternVL3 (Zhu et al. 2025)	8B	80.8	47.4	54.4	38.7
PDF-WuKong (Xie et al. 2024)	8.5B	76.9	<u>56.1</u>	-	-
Qwen2.5-VL (Bai et al. 2025)	3B	84.4	50.6	59.1	40.0
Qwen2.5-VL (Bai et al. 2025)	7B	<u>87.2</u>	55.0	<u>66.4</u>	<u>51.1</u>
URaG-3B (ours)	3B	86.0	54.1	63.8	41.5
URaG-7B (ours)	7B	**88.2**	**57.6**	**72.1**	**52.2**

Table 2: Performance comparison with different methods on MPDocVQA, DUDE, SlideVQA, and LongDocURL benchmarks.

Method	#Param	Evidence Modalities					Evidence Locations			Overall	
		TXT	LAY	CHA	TAB	IMG	SIN	MUL	UNA	ACC	F1
DeepSeek-VL (Lu et al. 2024)	7B	7.2	6.5	1.6	5.2	7.6	5.2	7.0	12.8	7.4	5.4
Idefics2 (Laurençon et al. 2024)	8B	9.0	10.6	4.8	4.1	8.7	7.7	7.2	5.0	7.0	6.8
MiniCPM-V2.5 (Yao et al. 2024)	8B	11.9	10.8	5.1	5.9	12.2	9.5	9.5	4.5	8.5	8.6
InternLM-XC2-4KHD (Dong et al. 2024)	8B	9.9	14.3	7.7	6.3	13.0	12.6	7.6	9.6	10.3	9.8
mPLUG-DocOwl 1.5 (Hu et al. 2024a)	8B	8.2	8.4	2.0	3.4	9.9	7.4	6.4	6.2	6.9	6.3
Qwen-VL(Bai et al. 2023)	10B	5.5	9.0	5.4	2.2	6.9	5.2	7.1	6.2	6.1	5.4
Monkey (Li et al. 2024b)	10B	6.8	7.2	3.6	6.7	9.4	6.6	6.2	6.2	6.2	5.6
CogVLM2-LLaMA3 (Hong et al. 2024)	19B	3.7	2.7	6.0	3.2	6.9	3.9	5.3	3.7	4.4	4.0
InternVL2.5 (Chen et al. 2024c)	4B	20.4	15.1	8.9	12.5	16.6	19.7	12.4	13.5	15.9	15.6
InternVL3 (Zhu et al. 2025)	8B	28.4	26.7	13.1	20.7	24.9	29.0	16.3	26.2	24.1	23.1
SV-RAG (Chen et al. 2025)	4B	26.3	22.1	<u>25.0</u>	20.7	25.2	34.0	10.6	15.7	23.0	24.2
M3DocRAG (Cho et al. 2024)	10B	<u>30.0</u>	23.5	18.9	20.1	20.8	32.4	14.8	5.8	21.0	22.6
Qwen2.5-VL (Bai et al. 2025)	3B	29.0	26.8	18.6	17.4	22.4	31.8	15.7	27.8	25.5	24.1
Qwen2.5-VL (Bai et al. 2025)	7B	<u>30.0</u>	<u>26.9</u>	22.4	20.6	<u>22.9</u>	33.4	**17.5**	24.7	26.2	25.1
URaG-3B (ours)	3B	27.9	24.2	23.4	<u>25.2</u>	21.4	<u>36.9</u>	13.5	**48.9**	<u>31.1</u>	<u>28.7</u>
URaG-7B (ours)	7B	**33.6**	**27.7**	**29.3**	**27.5**	**27.2**	**42.7**	<u>16.9</u>	<u>43.5</u>	**33.8**	**32.8**

Table 3: Performance comparison with different methods on MMLongBench-Doc. Generalized accuracy across 5 evidence sources: pure text (TXT), layout (LAY), charts (CHA), tables (TAB), and images (IMG). Results are further categorized by the number of evidence pages: single-page (SIN), cross-page (MUL), and unanswerable (UNA) questions.

SlideVQA and MMLongBench-Doc, which contain substantially long inputs with average lengths of 20 and 47.5 pages, respectively. This highlights the robustness and scalability of URaG in handling extended document contexts. Secondly, from the perspective of evidence types, URaG shows superior performance on single-page questions, indicating that evidence localized within a single page is more accurately retrieved. This can also be attributed to the distribution of training data, where questions with single-page evidence are more prevalent. Thirdly, URaG performs particularly well on visually intensive question types such as charts (CHA) and images (IMG). This indicates the effectiveness of the cross-modal retrieval module in performing

semantic matching between textual and visual content.

Comparison with Baseline Method

To ensure a fair comparison, we fine-tune the baseline model (Bai et al. 2025) using the same training data and settings as URaG. As shown in Table 11, our method significantly outperforms the baseline, demonstrating its effectiveness. Notably, even without any fine-tuning of the MLLM backbone, by simply inserting a pretrained retrieval module, URaG already surpasses the fully fine-tuned baseline. This highlights the strength of our cross-modal retrieval module, which effectively exploits the MLLM's inherent evidence localization ability to perform retrieval. With this

Method	SlideVQA	MMLong	LongDoc
Baseline	59.1	25.5	40.0
Baseline w/ SFT	61.9	29.1	37.3
URaG-3B w/o finetune	62.1	29.4	**43.1**
URaG-3B	**63.8**	**31.1**	41.5

Table 4: Comparison with baseline method. MMLong and LongDoc refer to MMLongBench-Doc and LongDocURL, respectively.

simple and lightweight design, URaG achieves strong performance without large-scale training. Moreover, on the LongDocURL dataset, fine-tuning leads to degraded performance. We attribute this to potential overfitting or domain mismatch between training and evaluation data. In contrast, URaG without any fine-tuning maintains robust performance, further demonstrating its generalization ability and practical applicability.

Ablation Study

The Position of Retrieval Module. We investigate the impact of inserting the cross-modal retrieval module at different layers of the LLM using the 3B-size model. As shown in Table 5, the results reveal that inserting the retrieval module at early to mid layers (e.g., layer 6) leads to the best overall performance. This can be attributed to two main factors. First, although the top1 retrieval accuracy continues to improve slightly at deeper layers (e.g., layer 12 or 18), the top5 accuracy already reaches saturation at layer 6, and moving the retrieval module deeper yields only marginal gains. Second, placing the retrieval module at earlier layers allows the subsequent LLM layers to concentrate on reasoning over a reduced set of visual features, effectively filtering out irrelevant information and improving the final answer generation quality. In summary, these results support our design choice: inserting the retrieval module at early layers captures sufficiently discriminative semantic representations for evidence selection, while leaving deeper layers to focus on reasoning.

Layer	SlideVQA				MMLong	
	Top1	Top5	EM*	EM	Top5	GACC
2	89.0	98.4	67.4	63.7	82.0	31.0
6	92.1	98.9	**68.5**	**63.8**	85.4	**31.1**
12	93.1	**99.2**	67.1	62.9	85.6	31.0
18	**93.5**	**99.2**	67.1	62.3	85.4	30.6

Table 5: Ablation study of the cross-modal retrieval module insertion at different layers within the LLM. * indicates metrics evaluated on the single-page subset of SlideVQA while retaining only the top-1 page after the retrieval module.

Two-stage Training Strategy. We conduct an ablation study to evaluate the effectiveness of our two-stage training strategy. As shown in Table 6, the results demonstrate that both the retrieval pretraining stage and the joint fine-tuning stage contribute to the final performance. Concretely, the re-

trieval capability of the model is limited without pretraining, as the retrieval module is trained from random initialization. Moreover, fine-tuning on the pretrained model further improves both retrieval accuracy and overall understanding.

Pretrain	Fintune	SlideVQA		MMLong	
		Top5	EM	Top5	GACC
✗	✓	98.5	62.6	82.0	30.7
✓	✗	98.8	62.1	84.0	29.4
✓	✓	**98.9**	**63.8**	**85.4**	**31.1**

Table 6: Ablation study of our two-stage training strategy. MMLong refers to MMLongBench-Doc.

Computational Efficiency

To evaluate the computational efficiency of URaG, we conduct experiments on the SlideVQA dataset, where each question is originally associated with 20 document pages. To simulate longer input sequences, we duplicate the pages for each question. We compare URaG with two representative approaches: the token-compression-based mPLUG-DocOwl2 (Hu et al. 2024b) and the external-retriever-based SV-RAG (Chen et al. 2025), by integrating their techniques into a common baseline. Model computational cost is measured in floating-point operations (FLOPs). As shown in Table 7, URaG achieves consistently higher computational efficiency on longer inputs compared with other methods. When the number of input pages increases from 20 to 100, URaG reduces FLOPs by 44.0% to 55.8% compared to the baseline. These results demonstrate the effectiveness of our method in reducing computational complexity for long document inputs. In addition, we analyze the number of parameters introduced by the cross-modal retrieval module and find that it accounts for only 0.05% to 0.07% of the total model parameters, which is nearly negligible.

Method	Pages		
	20	60	100
Baseline	415.9	1246.4	2076.9
mPLUG-DocOwl2 (2024b)	**208.3**	624.5	1040.7
SV-RAG (2025)	393.1	969.5	1546.0
URaG-7B (ours)	232.8	**574.9**	**917.0**
Reduction	-44.0%	-53.9%	-55.8%

Table 7: Computational efficiency comparison with different methods in terms of FLOPs (T).

Conclusion

In this paper, we propose URaG, a unified framework that unifies retrieval and generation within a single multimodal large language model (MLLM) for efficient long document understanding. URaG introduces a lightweight cross-modal retrieval module that explicitly leverages the inherent evidence localization capabilities of early layers of MLLMs,

enabling it to identify and retain only the most relevant pages during the reasoning process. Extensive experiments across multiple long document understanding benchmarks demonstrate that URaG not only achieves state-of-the-art performance but also significantly reduces computational overhead by 44-56%. We believe this work not only provides a practical solution but also valuable insights into a novel paradigm for long document understanding.

Acknowledgments

References

Abdin, M.; Aneja, J.; Awadalla, H.; Awadallah, A.; Awan, A. A.; Bach, N.; Bahree, A.; Bakhtiari, A.; Bao, J.; Behl, H.; et al. 2024. Phi-3 technical report: A highly capable language model locally on your phone. *arXiv preprint arXiv:2404.14219*.

Appalaraju, S.; Tang, P.; Dong, Q.; Sankaran, N.; Zhou, Y.; and Manmatha, R. 2024. DocFormerv2: Local features for document understanding. In *Proc. AAAI*, volume 38, 709–718.

Bai, J.; Bai, S.; Chu, Y.; Cui, Z.; Dang, K.; Deng, X.; Fan, Y.; Ge, W.; Han, Y.; Huang, F.; et al. 2023. Qwen technical report. *arXiv preprint arXiv:2309.16609*.

Bai, S.; Chen, K.; Liu, X.; Wang, J.; Ge, W.; Song, S.; Dang, K.; Wang, P.; Wang, S.; Tang, J.; et al. 2025. Qwen2.5-VL technical report. *arXiv preprint arXiv:2502.13923*.

Beyer, L.; Steiner, A.; Pinto, A. S.; Kolesnikov, A.; Wang, X.; Salz, D.; Neumann, M.; Alabdulmohsin, I.; Tschannen, M.; Bugliarello, E.; et al. 2024. PaliGemma: A versatile 3B VLM for transfer. *arXiv preprint arXiv:2407.07726*.

Blau, T.; Fogel, S.; Ronen, R.; Golts, A.; Ganz, R.; Ben Avraham, E.; Aberdam, A.; Tsiper, S.; and Litman, R. 2024. GRAM: Global reasoning for multi-page VQA. In *Proc. CVPR*, 15598–15607.

Chen, J.; Xiao, S.; Zhang, P.; Luo, K.; Lian, D.; and Liu, Z. 2024a. BGE M3-Embedding: Multilingual, multi-functionality, multi-granularity text embeddings through self-knowledge distillation. *arXiv preprint arXiv:2402.03216*.

Chen, J.; Zhang, R.; Zhou, Y.; Yu, T.; Dernoncourt, F.; Gu, J.; Rossi, R. A.; Chen, C.; and Sun, T. 2025. SV-RAG: LoRA-contextualizing adaptation of large multimodal models for multi-page document Understanding. In *Proc. ICLR*.

Chen, Z.; Wang, W.; Cao, Y.; Liu, Y.; Gao, Z.; Cui, E.; Zhu, J.; Ye, S.; Tian, H.; Liu, Z.; et al. 2024b. Expanding performance boundaries of open-source multimodal models with model, data, and test-time scaling. *arXiv preprint arXiv:2412.05271*.

Chen, Z.; Wu, J.; Wang, W.; Su, W.; Chen, G.; Xing, S.; Zhong, M.; Zhang, Q.; Zhu, X.; Lu, L.; et al. 2024c. InternVL: Scaling up vision foundation models and aligning for generic visual-linguistic tasks. In *Proc. CVPR*, 24185–24198.

Cho, J.; Mahata, D.; Irsoy, O.; He, Y.; and Bansal, M. 2024. M3DocRAG: Multi-modal retrieval is what you need for multi-page multi-document understanding. *arXiv preprint arXiv:2411.04952*.

Cui, C.; Sun, T.; Lin, M.; Gao, T.; Zhang, Y.; Liu, J.; Wang, X.; Zhang, Z.; Zhou, C.; Liu, H.; Zhang, Y.; Lv, W.; Huang, K.; Zhang, Y.; Zhang, J.; Zhang, J.; Liu, Y.; Yu, D.; and Ma, Y. 2025. PaddleOCR 3.0 Technical Report. arXiv:2507.05595.

Deng, C.; Yuan, J.; Bu, P.; Wang, P.; Li, Z.-Z.; Xu, J.; Li, X.-H.; Gao, Y.; Song, J.; Zheng, B.; et al. 2024. LongDocURL: a comprehensive multimodal long document benchmark integrating understanding, reasoning, and locating. *arXiv preprint arXiv:2412.18424*.

Devlin, J.; Chang, M.-W.; Lee, K.; and Toutanova, K. 2019. BERT: Pre-training of deep bidirectional Transformers for language understanding. In *Proc. NAACL*, 4171–4186.

Dong, Q.; Kang, L.; and Karatzas, D. 2024. Multi-page document VQA with recurrent memory Transformer. In *Proc. ICDAR Workshop*, 57–70. Springer.

Dong, X.; Zhang, P.; Zang, Y.; Cao, Y.; Wang, B.; Ouyang, L.; Zhang, S.; Duan, H.; Zhang, W.; Li, Y.; et al. 2024. InternLM-XComposer2-4KHD: A pioneering large vision-language model handling resolutions from 336 pixels to 4K HD. *Proc. NeurIPS*, 37: 42566–42592.

Faysse, M.; Sibille, H.; Wu, T.; Omrani, B.; Viaud, G.; Hudelot, C.; and Colombo, P. 2025. Colpali: Efficient document retrieval with vision language models. In *Proc. ICLR*.

Hong, W.; Wang, W.; Ding, M.; Yu, W.; Lv, Q.; Wang, Y.; Cheng, Y.; Huang, S.; Ji, J.; Xue, Z.; et al. 2024. CogVLM2: Visual language models for image and video understanding. *arXiv preprint arXiv:2408.16500*.

Hu, A.; Xu, H.; Ye, J.; Yan, M.; Zhang, L.; Zhang, B.; Li, C.; Zhang, J.; Jin, Q.; Huang, F.; et al. 2024a. mPLUG-DocOwl 1.5: Unified structure learning for ocr-free document understanding. *arXiv preprint arXiv:2403.12895*.

Hu, A.; Xu, H.; Zhang, L.; Ye, J.; Yan, M.; Zhang, J.; Jin, Q.; Huang, F.; and Zhou, J. 2024b. mPLUG-DocOwl2: High-resolution compressing for OCR-free multi-page document understanding. *arXiv preprint arXiv:2409.03420*.

Hu, E. J.; Shen, Y.; Wallis, P.; Allen-Zhu, Z.; Li, Y.; Wang, S.; Wang, L.; Chen, W.; et al. 2022. LoRA: Low-rank adaptation of large language models. In *Proc. ICLR*.

Huang, Y.; Lv, T.; Cui, L.; Lu, Y.; and Wei, F. 2022. LayoutLMv3: Pre-training for document ai with unified text and image masking. In *Proc. ACM MM*, 4083–4091.

Jia, M.; Yu, W.; Ma, K.; Fang, T.; Zhang, Z.; Ouyang, S.; Zhang, H.; Jiang, M.; and Yu, D. 2024. Leopard: A vision language model for text-rich multi-image tasks. *arXiv preprint arXiv:2410.01744*.

Karpukhin, V.; Oguz, B.; Min, S.; Lewis, P. S.; Wu, L.; Edunov, S.; Chen, D.; and Yih, W.-t. 2020. Dense passage retrieval for open-domain question answering. In *Proc. EMNLP*, 6769–6781.

Khattab, O.; and Zaharia, M. 2020. ColBERT: Efficient and effective passage search via contextualized late interaction over BERT. In *Proc. SIGIR*, 39–48.

Laurençon, H.; Saulnier, L.; Tronchon, L.; Bekman, S.; Singh, A.; Lozhkov, A.; Wang, T.; Karamcheti, S.; Rush, A.; Kiela, D.; et al. 2023. OBELICS: An open web-scale filtered dataset of interleaved image-text documents. *Proc. NeurIPS*, 36: 71683–71702.

Laurençon, H.; Tronchon, L.; Cord, M.; and Sanh, V. 2024. What matters when building vision-language models? *Proc. NeurIPS*, 37: 87874–87907.

Lee, C.; Roy, R.; Xu, M.; Raiman, J.; Shoeybi, M.; Catanzaro, B.; and Ping, W. 2024. Nv-Embed: Improved techniques for training LLMs as generalist embedding models. *arXiv preprint arXiv:2405.17428*.

León, J. A.; Moreno, J. D.; Escudero, I.; and Kaakinen, J. K. 2019. Selective attention to question-relevant text information precedes high-quality summaries: Evidence from eye movements. *Journal of Eye Movement Research*, 12(1): 10–16910.

Li, F.; Zhang, R.; Zhang, H.; Zhang, Y.; Li, B.; Li, W.; Ma, Z.; and Li, C. 2024a. LLaVA-NeXT-Interleave: Tackling multi-image, video, and 3D in large multimodal models. *arXiv preprint arXiv:2407.07895*.

Li, Z.; Yang, B.; Liu, Q.; Ma, Z.; Zhang, S.; Yang, J.; Sun, Y.; Liu, Y.; and Bai, X. 2024b. Monkey: Image resolution and text label are important things for large multi-modal models. In *Proc. CVPR*, 26763–26773.

Lin, S.-C.; Lee, C.; Shoeybi, M.; Lin, J.; Catanzaro, B.; and Ping, W. 2025. MM-Embed: Universal Multimodal Retrieval with Multimodal LLMs. In *Proc. ICLR*.

Lu, H.; Liu, W.; Zhang, B.; Wang, B.; Dong, K.; Liu, B.; Sun, J.; Ren, T.; Li, Z.; Yang, H.; et al. 2024. DeepSeek-VL: towards real-world vision-language understanding. *arXiv preprint arXiv:2403.05525*.

Ma, X.; Lin, S.-C.; Li, M.; Chen, W.; and Lin, J. 2024a. Unifying multimodal retrieval via document screenshot embedding. *arXiv preprint arXiv:2406.11251*.

Ma, Y.; Zang, Y.; Chen, L.; Chen, M.; Jiao, Y.; Li, X.; Lu, X.; Liu, Z.; Ma, Y.; Dong, X.; et al. 2024b. MMLongBench-Doc: Benchmarking long-context document understanding with visualizations. *Proc. NeurIPS*, 37: 95963–96010.

Meta AI. 2024. LLaMA 3.2: Revolutionizing Edge AI and Vision with Open, Customizable Models. https://ai.meta.com/blog/llama-3-2-connect-2024-vision-edge-mobile-devices/.

Radford, A.; Kim, J. W.; Hallacy, C.; Ramesh, A.; Goh, G.; Agarwal, S.; Sastry, G.; Askell, A.; Mishkin, P.; Clark, J.; et al. 2021. Learning transferable visual models from natural language supervision. In *Proc. ICML*, 8748–8763. PmLR.

Raffel, C.; Shazeer, N.; Roberts, A.; Lee, K.; Narang, S.; Matena, M.; Zhou, Y.; Li, W.; and Liu, P. J. 2020. Exploring the limits of transfer learning with a unified text-to-text Transformer. *Journal of machine learning research*, 21(140): 1–67.

Reimers, N.; and Gurevych, I. 2019. Sentence-BERT: Sentence embeddings using siamese BERT-networks. In *Proc. EMNLP*, 3982–3992.

Robertson, S. E.; Walker, S.; Jones, S.; Hancock-Beaulieu, M. M.; Gatford, M.; et al. 1995. Okapi at TREC-3. *Nist Special Publication Sp*, 109: 109.

Salton, G.; Fox, E. A.; and Wu, H. 1983. Extended boolean information retrieval. *Communications of the ACM*, 26(11): 1022–1036.

Tanaka, R.; Nishida, K.; Nishida, K.; Hasegawa, T.; Saito, I.; and Saito, K. 2023. SlideVQA: A dataset for document visual question answering on multiple images. In *Proc. AAAI*, volume 37, 13636–13645.

Tito, R.; Karatzas, D.; and Valveny, E. 2023. Hierarchical multimodal Transformers for multipage DocVQA. *Pattern Recognition*, 144: 109834.

Van Landeghem, J.; Tito, R.; Borchmann, Ł.; Pietruszka, M.; Joziak, P.; Powalski, R.; Jurkiewicz, D.; Coustaty, M.; Anckaert, B.; Valveny, E.; et al. 2023. Document understanding dataset and evaluation (DUDE). In *Proc. ICCV*, 19528–19540.

Wang, P.; Bai, S.; Tan, S.; Wang, S.; Fan, Z.; Bai, J.; Chen, K.; Liu, X.; Wang, J.; Ge, W.; et al. 2024. Qwen2-VL: Enhancing vision-language model's perception of the world at any resolution. *arXiv preprint arXiv:2409.12191*.

Xiao, S.; Liu, Z.; Zhang, P.; Muennighoff, N.; Lian, D.; and Nie, J.-Y. 2024. C-Pack: Packed resources for general Chinese embeddings. In *Proc. SIGIR*, 641–649.

Xie, X.; Yan, H.; Yin, L.; Liu, Y.; Ding, J.; Liao, M.; Liu, Y.; Chen, W.; and Bai, X. 2024. WuKong: A large multimodal model for efficient long PDF reading with end-to-end sparse sampling. *arXiv preprint arXiv:2410.05970*.

Yao, Y.; Yu, T.; Zhang, A.; Wang, C.; Cui, J.; Zhu, H.; Cai, T.; Li, H.; Zhao, W.; He, Z.; et al. 2024. MiniCPM-V: A GPT-4V level MLLM on your phone. *arXiv preprint arXiv:2408.01800*.

Zhai, X.; Mustafa, B.; Kolesnikov, A.; and Beyer, L. 2023. Sigmoid loss for language image pre-training. In *Proc. ICCV*, 11975–11986.

Zhang, J.; Yu, Y.; and Zhang, Y. 2024. CREAM: Coarse-to-fine retrieval and multi-modal efficient tuning for document VQA. In *Proc. ACM MM*, 925–934.

Zhu, J.; Wang, W.; Chen, Z.; Liu, Z.; Ye, S.; Gu, L.; Tian, H.; Duan, Y.; Su, W.; Shao, J.; et al. 2025. InternVL3: Exploring advanced training and test-time recipes for open-source multimodal models. *arXiv preprint arXiv:2504.10479*.

Zou, J.; Zhang, Y.; Li, J.; Tian, X.; and Ding, N. 2023. Human attention during goal-directed reading comprehension relies on task optimization. *Elife*, 12: RP87197.

Appendix

Details of Analysis

Due to the constraints of computational resources, for samples with more than 10 pages, we crop them to a continuous span of 10 pages. Additionally, we adjust the configurations to control the resolution of the input image: the "max_pixels" is set to 200,704 for Qwen2.5-VL (Bai et al. 2025), and the "max_num" is set to 1 for InternVL2.5 (Chen et al. 2024b). The attention entropy is computed as follows:

$$p_i = \frac{w_i}{\sum_j w_j}, \tag{6}$$

$$entropy = -\sum_i p_i \log(p_i), \tag{7}$$

where w_i denotes the attention weight assigned to page i. Specifically, it is computed as follows.

$$w_i = \sum_{h=1}^{H} \sum_{v \in \text{Page}_i} A_{g,v}^{(l,h)} \tag{8}$$

where $A_{g,t}^{(l,h)}$ denotes the attention score from the generated token g to token v at layer l and head h, H is the total number of attention heads, and Page_i denotes the set of token indices belonging to page i. The embedding similarity is computed following Equation (1) in the Methodology section of the main paper. We further report the results on the MMLongBench-Doc (Ma et al. 2024b) benchmark, as shown in Figure 4, which provides further empirical support for the analysis discussed in the main paper.
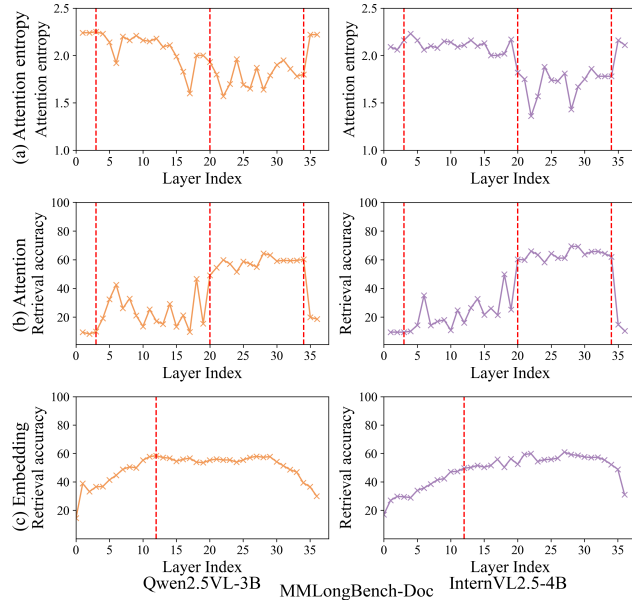

Figure 4: Analysis of MLLMs on long document understanding. (a) Attention entropy. (b) Attention-based retrieval accuracy. (c) Embedding-based retrieval accuracy.

Details of Computational Efficiency

We compare URaG with two representative approaches by integrating their techniques into a common baseline: the token-compression-based mPLUG-DocOwl2 (Hu et al. 2024b) and the external-retriever-based SV-RAG (Chen et al. 2025). Specifically, for mPLUG-DocOwl2, we incorporate the high-resolution DocCompressor module after the vision encoder of Qwen2.5VL (Bai et al. 2025) to reduce the sequence length of each document image to 324 tokens, and compute the overall FLOPs. For SV-RAG, we follow its original design by adding two separate sets of LoRA (Hu et al. 2022) adapters to Qwen2.5VL to construct the retriever and generator, respectively. All document pages are processed by the retriever, and the retrieved top-5 pages are sent to the generator. The total computational cost is computed by summing the FLOPs of both modules. In addition, we report results for the 3B-size variant of each method. As shown in Table 8, URaG-3B consistently achieves higher computational efficiency under longer inputs. When the number of input pages increases from 20 to 100, URaG-3B reduces FLOPs by 34.8% to 44.0% compared to the baseline. These results further highlight the computational efficiency of URaG.

Method	Pages		
	20	60	100
Baseline	243.5	730.0	1215.2
mPLUG-DocOwl2 (2024b)	**152.4**	457.0	761.6
SV-RAG (2025)	230.3	568.5	906.6
URaG-3B (ours)	158.9	**419.5**	**680.2**
Reduction	-34.8%	-42.5%	-44.0%

Table 8: Computational efficiency comparison with different methods in terms of FLOPs (T).

Method	#Params		Proportion (%)
	Retrieval Module	Total	
URaG-3B	2.5M	3.5B	0.07
URaG-7B	4.0M	7.7B	0.05

Table 9: Proportion of the cross-modal retrieval module parameters in total model size.

Parameter Efficiency

As shown in Table 9, we analyze the number of parameters introduced by the cross-modal retrieval module and find that it accounts for only 0.05% to 0.07% of the total model parameters, which is nearly negligible.

Additional Implementation Details

To limit the sequence length of visual tokens, we set the hyperparameters "min_pixels" and "max_pixels" as 100,352

and 802,816, respectively. During inference, we set the temperature to 1.0 and top-p to 1.0. The random seed is fixed to 42 across the experiments to ensure reproducibility.

Additional Experiences of Computational Efficiency

We record the average inference time per question and the peak GPU memory usage. As shown in Table 10, when the number of input pages increases from 20 to 100, our method achieves a time reduction of 16.7% to 41.6% and a memory reduction of 31.1% to 51.3% compared to the baseline. These results demonstrate the effectiveness of our method in accelerating inference and reducing memory consumption.

Method	Page	Time(s)	Mem(GB)
Qwen2.5VL	20	3.66	14.30
URaG(ours)	20	3.05 (-16.67%)	9.85 (-31.12%)
Qwen2.5VL	40	8.67	21.40
URaG(ours)	40	6.11 (-29.53%)	12.61 (-41.07%)
Qwen2.5VL	60	15.62	28.51
URaG(ours)	60	9.80 (-37.26%)	15.34 (-46.19%)
Qwen2.5VL	80	24.35	35.62
URaG(ours)	80	13.82 (-43.24%)	18.07 (-49.27%)
Qwen2.5VL	100	32.07	42.73
URaG(ours)	100	18.74 (-41.57%)	20.81 (-51.30%)

Table 10: Additional Efficiency comparison of URaG and baseline model.

Additional Experiments

To validate the generalizability of our proposed framework, we implement URaG based on InternVL2.5-4B (Chen et al. 2024b), and train it using the same data and settings described in the main paper. The results are shown in Table 11, our method outperforms the baseline across multiple benchmarks, demonstrating the effectiveness and versatility of the proposed framework.

Method	SlideVQA	MMLong	LongDocURL
Baseline	45.2	15.9	24.0
URaG-4B	**51.9**	**16.8**	**29.5**

Table 11: Comparison URaG-4B with baseline method. MMLong refers to MMLongBench-Doc.

Visualization of Retrieval

To better understand the retrieval behavior of our method, we visualize the patch-level embedding similarity between the query and document pages using URaG-7B. As shown in Figure 5 and 6, the model effectively identifies relevant regions corresponding to the query. For instance, for the question "How many people are standing in front of the chalkboard in the photograph?", the model highlights visual regions associated with "people" and the "chalkboard". For
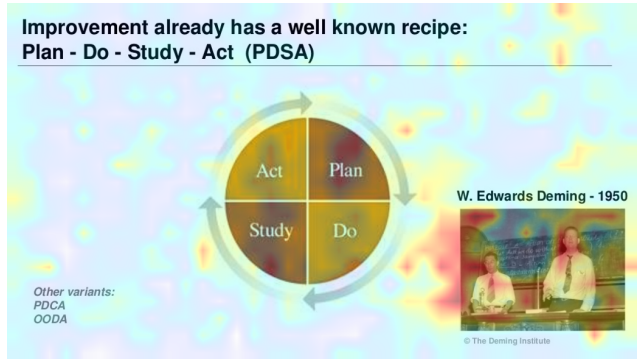
Figure 5: Similarity heatmap for the query: "How many people are standing in front of the chalkboard in the photograph?".

the question "What are landslides?", the model accurately locates the keyword "landslides". These results indicate that the hidden states of the MLLMs encode fine-grained semantic alignment between the query and the visual content during reasoning. Our retrieval module effectively exploits these capabilities to perform evidence retrieval.
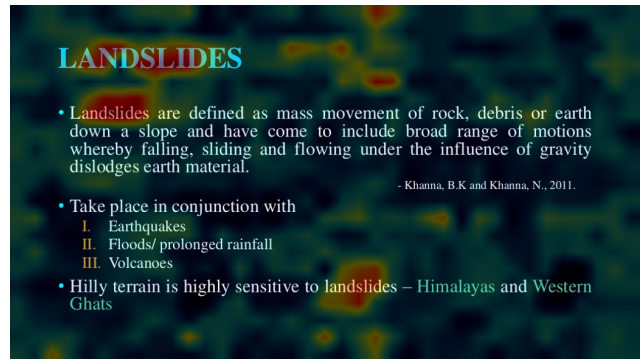

Figure 6: Similarity heatmap for the query: "What are landslides?".

Qualitative Results

As illustrated in Figure 7, URaG effectively extracts key information from long documents spanning dozens of pages, whether they are visually rich or text-dense.

Limitation

URaG employ a fixed top-k retrieval strategy, where k is set to 5 by default. In cases where crucial evidence is dispersed across more than k pages or concentrated within fewer pages, such a rigid selection could either omit essential information or introduce redundant inputs, thereby affecting both retrieval completeness and generation efficiency. A potential direction for future work is to design a dynamic or adaptive retrieval mechanism that adjusts k based on query difficulty or similarity confidence.
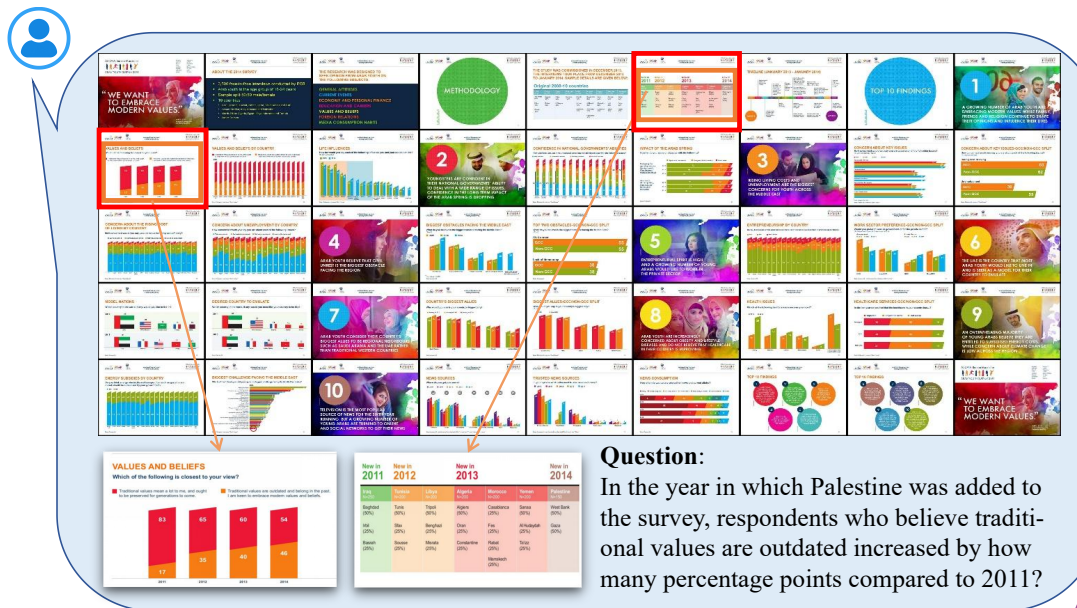
Question: In the year in which Palestine was added to the survey, respondents who believe traditional values are outdated increased by how many percentage points compared to 2011?

The percentage of respondents who believed traditional values are outdated increased by **29** percentage points compared to 2011.

URaG
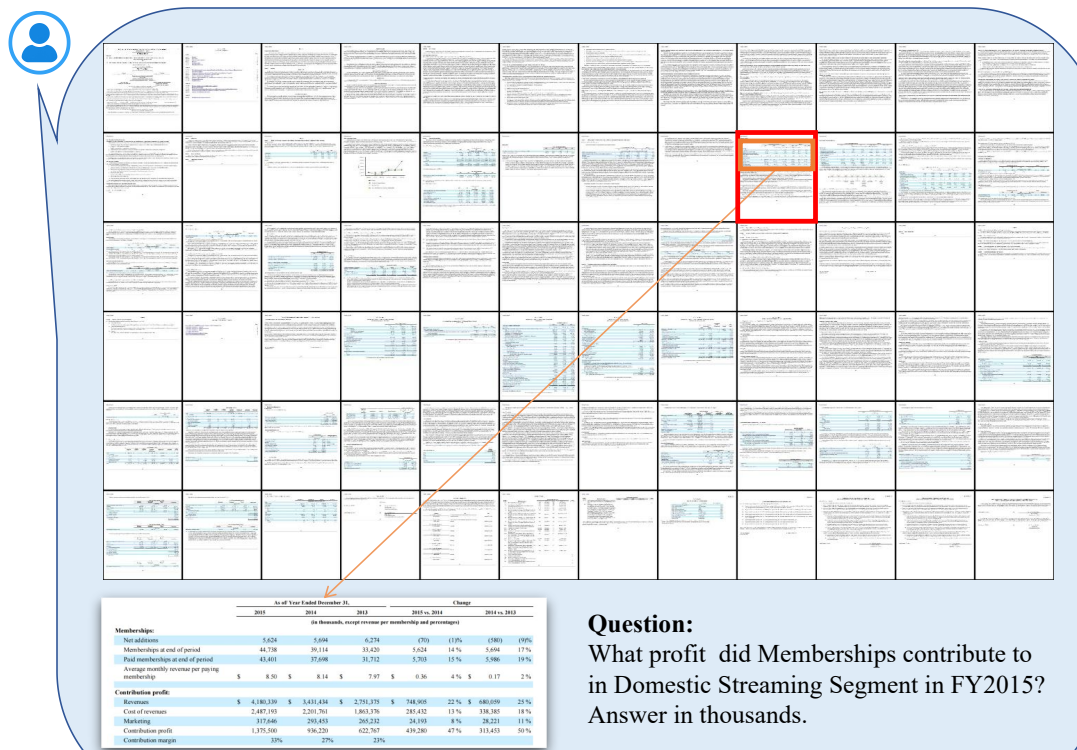
Question: What profit did Memberships contribute to in Domestic Streaming Segment in FY2015? Answer in thousands.

In FY 2015, Memberships contributed **$1,375,500** thousand to the profit of the Domestic Streaming segment.

URaG

Figure 7: Qualitative results of our URaG.